*Transactions of the Materials Research Society of Japan* 24 [4] 587-590 (1999)

# Bidirectional Temperature Response of Shape Memory Composites

Katsuya YASUMOTO and Hitoshi YOSHIDA*
National Institute of Materials and Chemical Research (NIMC), AIST, MITI,
1-1 Higashi, Tsukuba, Ibaraki 305-8565, JAPAN
Fax: 81-298-54-6298, e-mail: yasumoto@home.nimc.go.jp,
*Fax: 81-298-54-6798, e-mail: hyoshida@home.nimc.go.jp

Shape memory composites (SMCs), a sort of semiintelligent material, show reversible shape change in response to environmental temperature. SMCs consist of Ti-Ni alloy effectors with unidirectional temperature responsiveness and elastic polymer matrices—carbon-fiber-reinforced thermoplastics (CFRTPs) or room-temperature vulcanization (RTV) resins. To study the bidirectional temperature response and responsive force accompanying SMC shape change, we fabricated and tested ribbon and coil specimens. Shape changes in coil specimens were measured at room and high temperatures, i.e. temperatures beyond the phase transformation point from martensite to austenite in Ti-Ni alloys. The ratios of experimental and calculated values for deformation length are very close to 1.0, and numerical results were fairly satisfactory. We also studied the application of SMCs to greenhouses and micromachines.

Key words: Ti-Ni shape memory alloy, elastic polymer, intelligent material, greenhouse, micromachine

## 1. INTRODUCTION

Intelligent materials possess inherent sensor, effector, and processor functions, responding intelligently to environmental conditions. As such, these materials are expected to play an important role in sustainable development in the 21th century.

Intelligent materials are classified into two types [1]—microscopically distributed and macroscopically distributed. Optical fiber, piezoelectric ceramics, shape memory alloys (SMAs), and electrorheological fluids are being studied as potential raw materials for macroscopically distributed intelligent materials.

SMAs have received attention, because of their deformability and repeatability. SMA applications are being studied for active fiberscopes [2], catheters [3], forceps [4], robots [5], ventilation and so on [6].

We developed shape memory composites (SMCs) as a semiintelligent material. SMCs consist of Ti-Ni SMA effectors and elastic polymer matricies—carbon-fiber-reinforced thermoplastics (CFRTPs) or room-temperature vulcanization (RTV) resins. Ti-Ni SMA alone has only a unidirectional temperature response. When the temperature of the SMC is elevated beyond the phase transformation temperature of the SMA, large amounts of energy are generated in the SMA and stored temporarily as strain energy in the elastic matrix. When the temperature goes below the SMA phase transformation temperature, strain energy restores the SMC to its original shape, giving its bidirectional shape response. We reported analytical theories on the bidirectional temperature response for ribbon specimens [7], so this paper focuses on coil specimens, explaining specimen preparation and comparing analytical theories with experimental values. We also touch on the application of ribbon and coil SMCs to greenhouses and micromachines.

## 2. ANALYTICAL THEORIES OF RESPONSE

The memorized length of the SMA coil at temperatures beyond SMA phase transformation is represented by $Lo$ and that of the initial length at room temperature by $Lo'$ (**Fig. 1 (a)** and **(b)**).

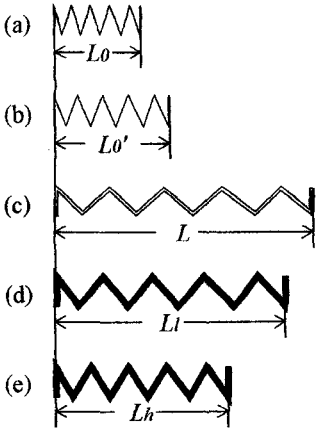


**Fig. 1** Coils

The SMA coil consists of a tubular matrix whose length is $L$ (**Fig. 1 (c)**). The length of the composite at low temperature is represented by $Ll$ and that of high temperature by $Lh$ (**Fig. 1 (d)** and **(e)**).

**Fig. 2** shows load-displacement diagrams. Line *a* is for the effector at low temperature, *b* that for high temperature, *c* that for the matrix at low temperature, and *d* that for high temperature.

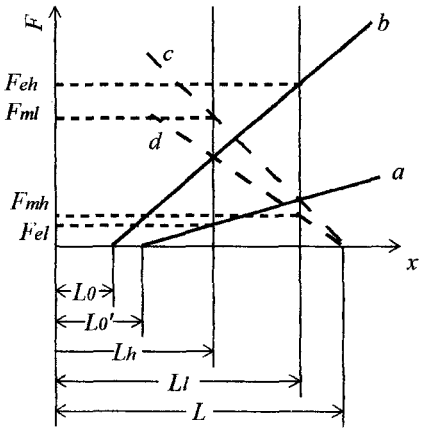


**Fig. 2** Load-displacement diagram

Because $L0$, $L0'$ and $L$ are known, we obtain the following equations for *a*, *b*, *c*, and *d*, if the inclinations of each line are given:

$$F = k_{el}(x - L_0') \quad , \tag{1}$$

$$F = k_{eh}(x - L_0) \quad , \tag{2}$$

$$F = -k_{ml}(x - L) \quad , \tag{3}$$

$$F = -k_{mh}(x - L) \quad , \tag{4}$$

where $kel$ and $keh$ are inclinations for the effector at low and high temperatures, and $kml$ and $kmh$ are inclinations for the matrix at low and high temperatures. When $x$ equals $Ll$ at low temperature, the force of eq. (1) equals that of eq. (3). The length of the composite at low temperature ($Ll$) is thus derived as follows:

$$L_l = \frac{k_{el}L_0' + k_{ml}L}{k_{el} + k_{ml}} \tag{5}$$

Similarly, the length of the composite at high temperature ($Lh$) is determined from eqs. (2) and (4) as follows:

$$L_h = \frac{k_{eh}L_0 + k_{mh}L}{k_{eh} + k_{mh}} \tag{6}$$

Strain energy $U$ stored in a coil spring is generally given as

$$U = \frac{F^2R^2l}{2GI_p} \quad , \tag{7}$$

where $F$, $G$, and $Ip$ are load, shearing modulus, and the polar moment of the inertia of the coil spring. $GIp$ is torsional rigidity. $R$ and $l$ are coil radius and total coil length. $l = 2\ \pi\ Rn$, where $n$ is the number of coil windings. Coil displacement is denoted as $\delta$, yielding the following equation for $\delta$ :

$$\delta = \frac{\partial U}{\partial F} = \frac{FR^2l}{GI_p} \tag{8}$$

For $F/\delta = k$, $k$ implies the load-displacement diagram inclination. $GIp$ is expressed using $k$ as follows:

$$GI_p = \frac{FR^2l}{\delta} = kR^2l \tag{9}$$

Because $R^2l$ is common to both the effector and matrix, eq. (9) becomes:

$$k_{ij} = \frac{G_{ij}I_{pi}}{R^2l} \quad , \qquad i = e, m, \qquad j = l, h \quad , \tag{10}$$

where $Gel$ and $Gml$ are the shearing modulus of the effector and matrix at low temperature, $Geh$ and $Gmh$ the shearing modulus of the effector and matrix at high temperature, and $Ipe$ and $Ipm$ the polar moment of the inertia of the effector and matrix. $GijIpi$ ($i = e, m, ; j = l, h$) are torsional rigidities for each cases. Substituting eq. (10) into eqs. (5) and (6), we obtain the following:

$$L_l = \frac{L_0'G_{el}I_{pe} + LG_{ml}I_{pm}}{G_{el}I_{pe} + G_{ml}I_{pm}} \quad , \tag{11}$$

$$L_h = \frac{L_0G_{eh}I_{pe} + LG_{mh}I_{pm}}{G_{eh}I_{pe} + G_{mh}I_{pm}} \tag{12}$$

These composite systems exhibit bidirectional shape deformation between $Ll$ and $Lh$ for environmental temperature change accompanying SMA effector phase transformation from martensite to austenite.

When the environmental temperature is elevated to the upper temperature ($Af$) of SMA effector phase transformation, when the length of $Ll$ is retained, forces generated in the effector and matrix are represented by

$F_{eh}$ and $F_{mh}$ (**Fig. 2**). The forces generated in the composite ($F_{ch}$) are given by the difference of $F_{eh}$ and $F_{mh}$. Substituting $L_l$ into $x$ in eqs. (2) and (4) yields the following expressions for $F_{eh}$, $F_{mh}$, and $F_{ch}$:

$$F_{eh} = k_{eh}(L_l - L_0) \quad , \tag{13}$$

$$F_{mh} = -k_{mh}(L_l - L) \quad , \tag{14}$$

$$\therefore F_{ch} \equiv F_{eh} - F_{mh} = k_{eh}(L_l - L_0) + k_{mh}(L_l - L) \quad . \tag{15}$$

Substituting eq. (10) into $k_{eh}$ and $k_{mh}$ of eq. (15) yields the following:

$$F_{ch} = \frac{G_{eh}I_{pe}}{R^2 l}(L_l - L_0) + \frac{G_{mh}I_{pm}}{R^2 l}(L_l - L) \quad . \tag{16}$$

When the environmental temperature falls below the phase transformation temperature ($A_s$) for the SMA effector, while retaining $L_h$, the forces generated in the effector and matrix are represented by $F_{el}$ and $F_{ml}$ (**Fig. 2**). Forces generated in the composite ($F_{cl}$) are derived similarly in eq. (16):

$$F_{cl} = \frac{G_{el}I_{pe}}{R^2 l}(L_h - L_0') + \frac{G_{ml}I_{pm}}{R^2 l}(L_h - L) \quad . \tag{17}$$

## 3. SPECIMEN PREPARATION

Ti-Ni SMA coils were heat-treated in air at 450 ℃ for 30 minutes for the SMA to memorize length $L_0$. The SMA coil was covered with fibrous textile acrylic tubes as resin-retention material. While maintaining the length of coil $L$, we spread RTV resins—silicone resin (KE-26, Shin-Etsu Chemical Co., Ltd.)—as the matrix on the coil. We used two types of Ti-Ni SMA wires, 0.5 mm and 1.0 mm in diameter (**Table** I ). For 0.5 mm SMA wire, the coil radius ($R$) is 7 mm, the memorized shape length of coil ($L_0$) 6 mm, the initial length of the effector at room temperature ($L_0'$) 15 mm, and the initial length of matrix ($L$) 140 mm. For 1.0 mm wire, $R$ is 12.5 mm, $L_0$ 15 mm, $L_0'$ 25 mm and $L$ 170 mm. The number of windings ($n$) is 8. The phase transformation temperatures of Ti-Ni SMA are $A_s$ (start temperature of phase transformation from martensite to austenite) = 50 ℃ and $A_f$ (finish temperature of phase transformation from martensite to austenite) = 60 ℃ for both SMA coils.

## 4. RESULTS AND DISCUSSION

**Fig. 3** shows an example of an SMC coil (a) at 60 ℃ and (b) at room temperature in water.

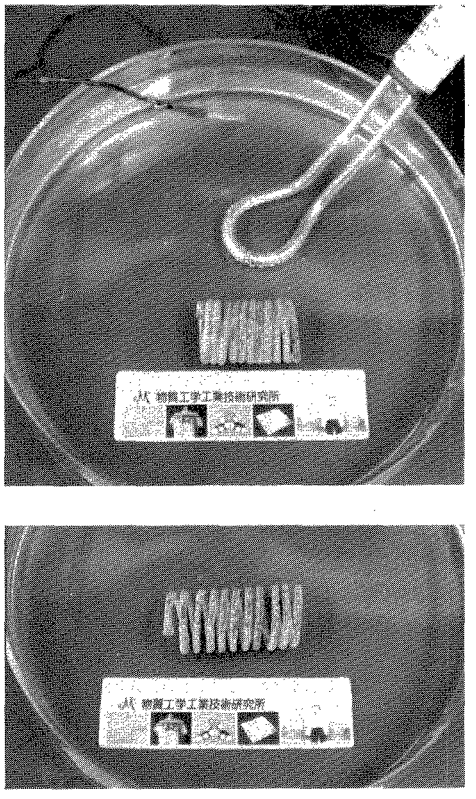

Fig. 3 Example of SMC coil
(a) at 60 ℃ ($L_h$ = 6.5 cm) and
(b) at room temperature ($L_l$ = 9 cm) in water

**Table** I shows the torsional rigidities of effectors and matrices calculated using eqs. (9) and (10) from the experimental load-displacement characteristics for each specimen.

**Table** I Torsional rigidity of coil specimens

| Specimen | Ti-Ni wire Diameter | Torsional rigidity $GI_p$ [Nmm$^2$] | | | |
|---|---|---|---|---|---|
| | | Effector | | Matrix | |
| | | 23 ℃ | 60 ℃ | 23 ℃ | 60 ℃ |
| 5-1 | 0.5 mm | 35.8 | 80.6 | 144 | 156 |
| 5-2 | | 26.9 | 84.8 | 269 | 270 |
| 10-1 | 1.0 mm | 1114 | 2715 | 2340 | 1727 |
| 10-2 | | 1248 | 3036 | 1836 | 1393 |
| 10-3 | | 1313 | 3096 | 2321 | 1798 |

**Table** II shows experimental and calculated values of specimen lengths ($L_l$, $L_h$) and their ratios. Length $L_l$ was measured at room temperature (23 ℃ ) and $L_h$ at 60 ℃ in a water bath. **Table** III shows the force generated with temperature change, measured by elevating the temperature where the retained length of SMC was $L_l$.

**Table** II Coil length at low and high temperatures

| | Room Temp. (23 ℃) | | | High Temp. (60 ℃) | | |
|---|---|---|---|---|---|---|
| | *Ll* [mm] | | | *Lh* [mm] | | |
| | Exper. Values ① | Calc. Values ② | Ratio ①/② | Exper. Values ③ | Calc. Values ④ | Ratio ③/④ |
| 5-1 | 118 | 126 | 0.94 | 101 | 101 | 1.00 |
| 5-2 | 110 | 126 | 0.87 | 88.7 | 107 | 0.83 |
| 10-1 | 97.4 | 99.2 | 0.98 | 70.5 | 67.8 | 1.04 |
| 10-2 | 92.2 | 84.9 | 1.09 | 65.2 | 56.2 | 1.16 |
| 10-3 | 105 | 120 | 0.88 | 75.0 | 82.6 | 0.91 |

**Table** III Force generated from room to high temperatures

| | *Fch* [N] | | |
|---|---|---|---|
| | Experimental Values ⑤ | Calculated Values ⑥ | Ratio ⑤/⑥ |
| 5-1 | 0.67 | 0.80 | 0.84 |
| 5-2 | 0.61 | 0.75 | 0.81 |
| 10-1 | 2.2 | 3.09 | 0.71 |
| 10-2 | 2.44 | 2.52 | 0.97 |
| 10-3 | 2.32 | 2.74 | 0.85 |

At room temperature, the ratios of experimental and calculated values for lengths of composite were within 0.87 to 1.09, and those at high temperature within 0.83 to 1.16, demonstrating that the analytical theories in our study are valid. For generated force, experimental values are smaller than the calculated in all specimens. There are constraint effects on the boundary face between the effector and matrix. For more exact design of the force generated, we must study the boundary between the effector and matrix.

In a 1/10 scale model of a greenhouse (a) at 45 ℃ and (b) at room temperature, we used the ribbon SMC with flexural response in a semicircular shape (**Fig. 4**) [7]. Only temperature control was possible. The growth of vegetables is influenced by environmental conditions, light, temperature, humidity, $CO_2$ concentration, and so on. Other environmental controls are needed for practical use. The smaller the SMC shape, the more heat capacity is reduced. The response speed will be improved. The application of SMC to micromachines is thus reasonable. We will miniaturize the coil SMC (**Fig. 3**) to use for micromachines.

## 5. CONCLUSIONS

We dealt mainly with coil SMCs. Analytical theories on SMC deformation length between low and high temperatures agreed with experimental values.

If we know the torsional rigidity and original length of raw materials, we can theoretically obtain the SMC deformation length. For SMC application, studies are under way for integrating sensors and miniaturizing SMCs. We eventually hope to apply SMCs to macro- and micro-size intelligent materials.

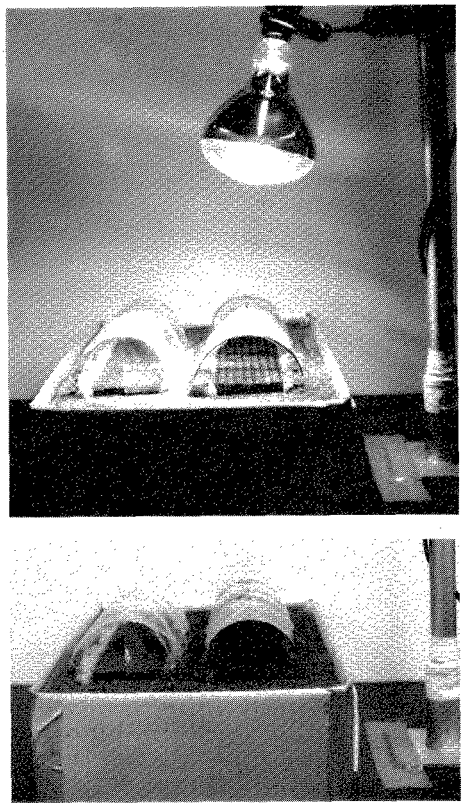

**Fig. 4** Greenhouse 1/10 scale model
(a) at 45 ℃ (open) and
(b) at room temperature (closed)

References

[1] N. Koshizaki, K. Yasumoto, S. Yano, and H. Yoshida, "Intelligent functionalities of composite materials", *Bulletin of Industrial Products Research Institute*, **127**, 99-128 (1992) (in Japanese).

[2] S. Maeda, O. Tohyama and H. Ito, *IEICE Trans. Electron.*, **E80-C, No. 2**, 226-231 (1997).

[3] T. Mineta, Y. Watanabe, S. Kobayashi, Y. Haga, and M. Esashi, *Technical Digest of the 16th Sensor Symposium*, 181-184 (1998).

[4] M. Hashimoto, T. Tokoda and T. Tabata, "Magnification of the motion area of SMA active forceps for laparoscopic surgery", *JSME ROBOMEC '97*, **B**, 1027-1030 (1997) (in Japanese).

[5] K. Nishikawa, J. Hakura, H. Yokoi, and Y. Kakazu, "A study on constructing symmetric body robot", *Proc. 15th Ann. Conf. Robot. Soc. of Jpn.*, **3**, 875-876 (1997) (in Japanese).

[6] For examples, see the following URLs as of Feb. 1999: http://www.ari.co.jp/factory/sentan/keijyo.html and http://www.nittan.co.jp/prd1201.htm (in Japanese).

[7] H. Yoshida, A. Funaki and S. Yano, *Adv. Composite Mater.*, **6-4**, 341-352 (1997).

(Received December 10, 1998; accepted April 14, 1999)